Pergamon

PII: S0045-7949(96)00382-3

Computers & Structures Vol. 63, No. 5, pp. 899–913, 1997

Printed in Great Britain
0045-7949/97 $17.00 + 0.00

ON THE ASSUMED STRAIN FORMULATION WITH SELECTIVE POLYNOMIAL ORDER ENRICHMENT FOR *p*-VERSION SHELLS

J. Fish and **R. Guttal**

Department of Civil Engineering and Scientific Computation Research Center, Rensselaer Polytechnic Institute, Troy, NY 12180, U.S.A.

(*Received* 20 *April* 1995)

Abstract—A family of hierarchical shell elements based on assumed strain formulation has been developed to enhance the performance of displacement-based hierarchical shell elements typically up to polynomial order six. For thin shells, hierarchical assumed strain elements with five degrees-of-freedom (two rotations and three mid-plane translations) and six degrees of freedom (three translations on the top and bottom surfaces of the shell) per hierarchical mode have been formulated. Hierarchical in-plane modes are adaptively selected on the basis of their ability to reduce solution errors. For thick shells both in-plane and through-the-thickness mode selection is controlled by the process of adaptivity. Numerical experiments have been carried out to test the usefulness of assumed strain formulation in the framework of the *p*-method combined with selective polynomial escalation. The sensitivity to element distortion and influence of super-parametric formulation on the rate of convergence have been numerically assessed.

1. INTRODUCTION

There have been two different philosophies concerning the optimal use of *p*-version of the finite element method:

(1) The early approach pioneered by Szabo and implemented in PROBE [1] advocates coarsest meshes consistent with the shape of the body for smooth solutions with practically unlimited polynomial order. The doctrine is motivated by the theoretical studies [2] indicating that exponential rate of convergence can be obtained with very coarse meshes if the solution is analytic and with meshes arranged in geometric progression for non-smooth solutions.
(2) Most recently several software houses, which in the past were primarily focusing on the *h*-version of the finite element method, have been driven by the market demands to integrate the *p*-version capabilities in their general purpose codes. Their approach has been to limit the element size so that a satisfactory solution quality can be obtained at a polynomial order no higher than four [3]. The primary reason for adopting such a point of view is based on the following two observations:

- At higher polynomial orders ($p \geqslant 5$) solution time is often dominated by the formation of the finite element matrices, especially in 3-D applications.
- Automatic coarse mesh generation consistent with each geometry for general applications is very difficult and currently such technology does not exist.

In an attempt to assess various computational strategies this paper focuses on computational aspects of the *p*-version of the finite element analysis of shells with emphasis on enhancing computational efficiency of higher-order hierarchical shell elements. The following two aspects are studied:

(1) How to enhance the performance of shell elements up to the polynomial order of 4–5 using assumed strain formulation [4].
(2) How to reduce the size of the element matrices by adaptively selecting higher-order modes [5].

2. ELEMENT FORMULATION

2.1. *Preliminaries*

Consider the geometry of a typical quadrilateral shell element defined by the following relation:

$$\mathbf{X} = \tfrac{1}{2}[(1+\xi_3)\mathbf{X}^{top}(\xi_1,\xi_2) + (1-\xi_3)\mathbf{X}^{bot}(\xi_1,\xi_2)] \quad (1)$$

where $\mathbf{X}$ denotes the position vector of a generic point of the shell in the global Cartesian coordinate system, $\mathbf{X}^{top}$ and $\mathbf{X}^{bot}$ are position vectors at the top and bottom surfaces, respectively. Equation (1) represents a smooth mapping of a biunit cube into physical shell

domain, with linear interpolation in ξ_3. $\xi_3 = 0$ corresponds to the middle surface of the shell. It is common in practice to interpolate the bottom and the top surfaces either using Lagrange polynomials [6], blending functions [7] or even Legendre polynomials [8].

The displacement field of a higher-order plate/shell theory can be approximated as in Refs [7, 9]

$$u_i = \sum_{\alpha=1}^{n_i} f_\alpha(\xi_3) u_{i\alpha}(\xi_1, \xi_2) \tag{2}$$

where $f_\alpha(\xi_3)$ in eqn (2) represents through-the-thickness variation of the displacement components. Typically, Legendre polynomials are chosen as basis functions for in-plane displacement components $u_{i\alpha}(\xi_1, \xi_2)$ to ensure numerical stability and hierarchiality.

The space spanned by hierarchic shape functions is denoted by $S^{(p,q)}$, where p is in-plane polynomial order of basis functions corresponding to the interpolation order of $u_{i\alpha}$ and q ($q \leqslant p$) is the polynomial order of basis functions in transverse direction identified with the polynomial order of $f_\alpha(\xi_3)$.

Shell element formulated on the basis of eqns (1) and (2) will be referred to as H3SOL—Hierarchical (3-*D*) Solid element. To enhance the performance of H3SOL for $q = 1$ plane stress assumption and shear correction factors are usually employed.

H3SOL is known to have the following drawbacks:

(1) Locking for lower-order elements and hence poor convergence. To circumvent this problem, we employ an assumed natural strain formulation. Thus, we introduce (see Section 2.2)

- Hierarchical (3-D) Assumed Natural Strain element that will be formally referred to as H3ANS. For $q = 1$ it employs plane stress assumption and shear correction factors. The formulation of this element is a specialization of the work by Stanley et al. [10] to the *p*-version.

(2) In thin shell limit, retention of 3 degrees-of-freedom at each node on top and bottom surfaces leads to large stiffness coefficients for relative displacements corresponding to shell thickness [10]. This leads to deterioration of the rate of convergence for lower polynomial orders. This phenomenon is especially prominent when thickness is small compared to the in-plane dimensions. To alleviate this drawback we propose either to reduce the stiffness in the transverse direction, or to employ hierarchical assumed natural strain degenerated element formulation with rotational degrees-of-freedom. Thus in Sections 2.3 and 2.4, we will describe the following types of elements:

- Hierarchical (3-D) Reduced transverse stiffness, assumed natural strain element denoted by H3RANS.
- Hierarchical (2-D) degenerated assumed natural strain element with rotational degrees-of-freedom denoted by H2ANS.
- For completeness we denote the Hierarchical (3-D) reduced transverse stiffness solid element by H3RSOL and a degenerated version of H3SOL will be denoted by H2SOL—Hierarchical (2-D)-degenerated solid element with rotational degrees-of-freedom.

H2-type elements have 5 degrees-of-freedom per hierarchical mode. They are used for thin and moderately thick shells. H3-type elements are intended to model very thin shell behavior as well as general compact solid behavior. They enable a uniform 3-D idealization of the problem domain that avoids 2-D/3-D transitions.

(3) In practice only a small fraction of hierarchical basis functions, spanning the space $S^{(p,q)}$, are needed to provide similar quality of the solution as the space spanned by monomials of degree p and q. The critical modes are selected on the basis of their ability to reduce the solution error [15]. Approximation spanned by these modes will be denoted by $S^{(p,q,l)}$, where l is the list of active hierarchical modes [17]. This process is very effective for the case of a single right-hand side vector. The pattern of polynomial order escalation would be different for each loading case, making the usefulness of this approach quite limited for general applications.

2.2. *H3ANS hierarchical (3-D) assumed natural strain element*

The element formulation is based on assumed strain interpolation in a natural coordinate system [10]. Displacement interpolation is carried out using Legendre polynomials, as in H3SOL. Element mapping is carried out using either blending functions or Lagrange polynomials.

2.2.1. *Definition of coordinate systems and basis vectors.* Let **X** be the global Cartesian coordinate system where geometry of the shell domain is defined and basis vectors $\mathbf{e}_i$ be the unit Cartesian vectors. Let ξ represent a natural element curvilinear coordinate system. Then the covariant basis vectors $\mathbf{a}_i$ and their contravariants $\mathbf{a}^i$ are defined as follows:

$$\mathbf{a}_i = \frac{\partial X_j}{\partial \xi_i}\mathbf{e}_j \quad \mathbf{a}^i = \frac{\partial \xi_i}{\partial X_j}\mathbf{e}_j \quad \mathbf{a}_i \cdot \mathbf{a}^j = \delta_i^j \tag{3}$$

Let **x** be the material Cartesian coordinate system where material properties of the element are defined. Plane stress assumption for classical shell theory ($q = 1$) is also exercised in this coordinate system. Unit basis vectors for the material coordinate system

are denoted by $\mathbf{p}_i$. They are defined such that, $\mathbf{p}_3$ is perpendicular to mid-surface and $\mathbf{p}_1$, $\mathbf{p}_2$ are as close as possible to $\mathbf{a}_1$, $\mathbf{a}_2$.

2.2.2. *Strain field in natural coordinate system of the element.* By the principle of invariance we have:

$$E_{ij}\mathbf{e}_i\mathbf{e}_j = \Xi_{ij}\mathbf{p}_i\mathbf{p}_j = \epsilon_{ij}\mathbf{a}^i\mathbf{a}^j \tag{4}$$

where E_{ij}, Ξ_{ij}, ϵ_{ij} are components of global, material and natural covariant strain tensor. Let $\mathbf{u} = u_i\,\mathbf{e}_i$ be the displacement vector. Then the strain tensor $\mathbf{E}$ is obtained by taking the symmetric gradient of the displacements, that is,

$$\mathbf{E} = \frac{1}{2}\left[\frac{\partial u_i}{\partial X_j} + \frac{\partial u_j}{\partial X_i}\right]\mathbf{e}_i\mathbf{e}_j = \epsilon_{ij}\mathbf{a}^i\mathbf{a}^j. \tag{5}$$

Contracting $\mathbf{E}$ by covariant curvilinear vectors $\mathbf{a}_i$, $\mathbf{a}_j$ and using eqn (3), yields the natural covariant strain tensor components

$$\epsilon_{ij} = \frac{1}{2}\left[\frac{\partial u_m}{\partial \xi_i}\frac{\partial X_m}{\partial \xi_j} + \frac{\partial u_n}{\partial \xi_j}\frac{\partial X_n}{\partial \xi_i}\right] = \frac{1}{2}[\mathbf{u}_{,\xi_i}\mathbf{a}_j + \mathbf{u}_{,\xi_j}\mathbf{a}_i]. \tag{6}$$

Let $\mathbf{N} \in S^{(p,4)}$ be the shape functions obtained using a tensor product of Legendre polynomials [7], then

$$\mathbf{u} = \sum_{A=1}^{\mathrm{NMDS}} N_A\mathbf{d}^A \tag{7}$$

where $\mathbf{d}$ is the displacement vector representing the amplitudes of hierarchical modes in the global coordinate system; NMDS is the number of modes, lower case subscripts denote space dimension, while upper case indices are reserved for mode numbering. Using eqn (6), the natural strain–displacement relation can now be recast as:

$$\epsilon = \sum_{A=1}^{\mathrm{NMDS}} \mathbf{B}_A^{\mathrm{nat}}\mathbf{d}^A \tag{8}$$

where

$$\mathbf{B}_A^{\mathrm{nat}} = \{b_{Aij}\} = \tfrac{1}{2}(N_{A,\xi_i}\mathbf{a}_j + N_{A,\xi_j}\mathbf{a}_i) \tag{9}$$

2.2.3. *Assumed natural strain field.* Given the polynomial orders $P_k(\epsilon_{ij})$ of strain field resulting from eqn (6), the polynomial order $\bar{P}_k(\bar{\epsilon}_{ij})$ of the assumed strain field in natural coordinate system $\bar{\epsilon}_{ij}$ is selectively reduced to alleviate membrane and shear locking primarily at lower polynomial orders using the following rule:

$$\bar{P}_k(\bar{\epsilon}_{ij}) = P_k(\epsilon_{ij}) - \delta_{\underline{i}\underline{k}}\delta_{\underline{j}\underline{k}} \tag{10}$$

δ_{ij} is a Kronecker delta, underlined subscripts indicate no sum over repeated indices.

We denote a set of reduced quadrature points by $(\bar{\xi}_1, \bar{\xi}_2, \bar{\xi}_3)$. A set of Lagrange shape functions $\bar{\Psi}(\xi)$ is defined with nodes at the reduced quadrature points. The assumed strain–displacement matrix $\bar{\mathbf{B}}_A$ is defined as:

$$\bar{\mathbf{B}}_A = \begin{Bmatrix} \bar{\mathbf{b}}_{A_{11}} \\ \bar{\mathbf{b}}_{A_{22}} \\ \bar{\mathbf{b}}_{A_{33}} \\ \bar{\mathbf{b}}_{A_{23}} \\ \bar{\mathbf{b}}_{A_{12}} \\ \bar{\mathbf{b}}_{A_{13}} \end{Bmatrix} \tag{11}$$

where

$$\bar{\mathbf{b}}_{A_{11}} = \sum_{i=1}^{NG\xi_1} N_{A,\xi_1}(\bar{\xi}_{1_i}, \xi_2, \xi_3)\mathbf{a}_1^{\mathrm{T}}(\bar{\xi}_{1_i}, \xi_2, \xi_3)\bar{\Psi}_i(\xi_1)$$

$$\bar{\mathbf{b}}_{A_{22}} = \sum_{j=1}^{NG\xi_2} N_{A,\xi_2}(\xi_1, \bar{\xi}_{2_j}, \xi_3)\mathbf{a}_2^{\mathrm{T}}(\xi_1, \bar{\xi}_{2j}, \xi_3)\bar{\Psi}_j(\xi_2)$$

$$\bar{\mathbf{b}}_{A_{33}} = \sum_{k=1}^{NG\xi_3} N_{A,\xi_3}(\xi_1, \xi_2, \bar{\xi}_{3_k})\mathbf{a}_3^{\mathrm{T}}(\xi_1, \xi_2, \bar{\xi}_{3_k})\bar{\Psi}_k(\xi_3)$$

$$\bar{\mathbf{b}}_{A_{23}} = \sum_{j=1}^{NG\xi_2}\sum_{k=1}^{NG\xi_3} [N_{A,\xi_3}(\xi_1, \bar{\xi}_{2_j}, \bar{\xi}_{3_k})\mathbf{a}_2^{\mathrm{T}}(\xi_1, \bar{\xi}_{2_j}, \bar{\xi}_{3_k}) + N_{A,\xi_2}(\xi_1, \bar{\xi}_{2_j}, \bar{\xi}_{3k})\mathbf{a}_3^{\mathrm{T}}(\xi_1, \bar{\xi}_{2_j}, \bar{\xi}_{3_k})] \times \bar{\Psi}_j(\xi_2)\bar{\Psi}_k(\xi_3)$$

$$\bar{\mathbf{b}}_{A_{12}} = \sum_{i=1}^{NG\xi_1}\sum_{j=1}^{NG\xi_2} [N_{A,\xi_1}(\bar{\xi}_{1_i}, \bar{\xi}_{2_j}, \xi_3)\mathbf{a}_2^{\mathrm{T}}(\bar{\xi}_{1_i}, \bar{\xi}_{2_j}, \xi_3) + N_{A,\xi_2}(\bar{\xi}_{1_i}, \bar{\xi}_{2j}, \xi_3)\mathbf{a}_1^{\mathrm{T}}(\bar{\xi}_{1_i}, \bar{\xi}_{2_j}, \xi_3)] \times \bar{\Psi}_i(\xi_1)\bar{\Psi}_j(\xi_2)$$

$$\bar{\mathbf{b}}_{A_{13}} = \sum_{i=1}^{NG\xi_1}\sum_{k=1}^{NG\xi_3} N_{A,\xi_1}(\bar{\xi}_{1_i}, \xi_2, \bar{\xi}_{3_k})\mathbf{a}_3^{\mathrm{T}}(\bar{\xi}_{1_i}, \xi_2, \bar{\xi}_{3_k}) + N_{A,\xi_3}(\bar{\xi}_{1_i}, \xi_2, \bar{\xi}_{3_k})\mathbf{a}_1^{\mathrm{T}}(\bar{\xi}_{1_i}, \xi_2, \bar{\xi}_{3_k})] \times \bar{\Psi}_i(\xi_1)\bar{\Psi}_k(\xi_3)$$

where $NG\xi_i$ is the number of reduced quadrature points in direction i.

2.2.4. *Stiffness matrix calculations*. Since the constitutive relations are expressed in material coordinate system, the natural strains are transformed to material coordinate system. From eqns (4) and (5), the strain components in material coordinate system are defined as:

$$\Xi_{kl} = \frac{\partial \xi_i}{\partial x_k}\frac{\partial \xi_j}{\partial x_l}\epsilon_{ij} = \left[\frac{\partial x_k}{\partial \xi_i}\right]^{-1}\left[\frac{\partial x_l}{\partial \xi_i}\right]^{-1}\epsilon_{ij} \equiv T_{klij}\epsilon_{ij} \quad (12)$$

or

$$\boldsymbol{\Xi} = \mathbf{T}\boldsymbol{\epsilon} \quad (13)$$

and the element stiffness matrix can be cast into the classical form:

$$\mathbf{K}^e = \int_\Omega \bar{\mathbf{B}}^T\mathbf{D}^e\bar{\mathbf{B}}\,d\Omega$$

where $\bar{\mathbf{B}}$ is defined by eqn (11) and

$$\mathbf{D}^e = \mathbf{T}^T\mathbf{D}^\Xi\mathbf{T}. \quad (14)$$

$\mathbf{D}^\Xi$ is the constitutive matrix defined in the material coordinate system.

2.2.5. *Remark*.

(1) Efficient implementation of H3ANS element involves formulation of interpolation and mapping functions as tensor product of functions in (ξ_1, ξ_2, ξ_3) directions. The basis functions $\mathbf{N}$ and mapping functions $\mathbf{H}$ can be expressed by,

$$\mathbf{N} = \phi_1(\xi_1)\phi_2(\xi_2)\phi_3(\xi_3) \quad (15)$$

$$\mathbf{H} = \mathbf{h}_1(\xi_1)\mathbf{h}_2(\xi_2) \quad (16)$$

and thus evaluation of the covariant basis vectors $\mathbf{a}_i$ and the $\bar{\mathbf{B}}$-matrix involves the derivatives of one-dimensional interpolants only.

2.3. *H3RANS—hierarchical (3-D) reduced transverse stiffness, assumed natural strain element*

For the purpose of examining the causes of somewhat stiffer behavior of H3-type elements compared to their degenerated counterparts [10], we consider a beam problem. For elastic isotropic beam the strain energy is given by,

$$U = \frac{1}{2}\int_L (D_B\kappa^2 + D_M\epsilon^2 + D_S\gamma^2)\,dx \quad (17)$$

where L is the element length; ϵ, κ and γ are the membrane strain, curvature and transverse shear strain, respectively; D_B, D_M and D_S are the bending, membrane and shear stiffness constants given by,

$$D_B = \frac{Et^3}{12} \quad D_M = Et \quad D_S = k_sGt \quad (18)$$

where t is the thickness of the beam of a unit width; E Young's modulus; G the shear modulus and k_s the shear correction factor.

In the classical beam formulation the normal strains μ are *a posteriori* calibrated to maintain zero normal stress (plane stress assumption), and thus have no contribution to the strain energy in eqn (17). It can be seen that as $t \to 0$ the bending energy becomes negligible in comparison to shear and membrane energy giving rise to shear and membrane locking, if the element cannot represent deformed state in which shear and membrane strains vanish throughout the element [11].

In H3-type beam elements normal strains are computed directly from kinematics. These values are not arbitrary and cannot be calibrated to maintain plane stress condition. Thus if two-dimensional state of stress is considered, the resulting strain energy takes the following form:

$$U = \frac{1}{2}\int_L (\bar{D}_B\kappa^2 + \bar{D}_M\epsilon^2 + \epsilon D_C\mu + D_S\gamma^2 + D_\mu\mu^2)\,dx \quad (19)$$

where

$$\bar{D}_M = \frac{D_M}{1-\nu^2} \quad \bar{D}_B = \frac{D_B}{1-\nu^2} \quad D_C = 2\nu\bar{D}_M$$

$$D_\mu = \bar{D}_M. \quad (20)$$

It can be seen that in H3-type flexural elements spurious coupling between membrane and normal deformation exists giving rise to a parasitic transverse normal strain energy, which is of the same order of magnitude as that of the membrane strain energy if the strains are of equal order. This phenomenon is referred here as the transverse normal locking of H3-type flexural elements.

To ameliorate the locking caused by the transverse normal strains we propose to calibrate the constitutive behavior of H3-type elements to match the strain energy corresponding to H2-type elements without introducing zero energy modes. By this technique the stiffness coefficients in the constitutive tensor are modified in the following way:

$$\bar{D}_M = D_M \quad \bar{D}_B = D_B \quad D_C = 0 \quad D_\mu = \chi D_M \quad (21)$$

where χ is a stabilization parameter aimed at stabilizing the zero transverse normal energy modes of H3-type flexural elements.

2.4. *H2SOL—hierarchic degenerated (2-D) solid element with rotational degrees-of-freedom*

In this section we attempt to formulate a degenerated assumed strain shell element, which employs blending functions or Lagrangian basis for geometry mapping and Legendre polynomials for solution interpolation.

As a starting point, the displacement field is expressed in terms of mid-point translations $u_i^t(\xi_1, \xi_2)$ and mid-point rotations $\theta_\alpha(\xi_1, \xi_2)$ which are defined with respect to the fiber coordinate system:

$$\begin{Bmatrix} u_1 \\ u_2 \\ u_3 \end{Bmatrix}_{(\xi_1,\xi_2,\xi_3)} = \begin{Bmatrix} u_1^t \\ u_2^t \\ u_3^t \end{Bmatrix}_{(\xi_1,\xi_2)} + \frac{\xi_3}{2}[-t\mathbf{e}_2^f, t\mathbf{e}_1^f]_{(\xi_1,\xi_2)} \begin{Bmatrix} \theta_1 \\ \theta_2 \end{Bmatrix} \quad (22)$$

where the unit vectors $(\mathbf{e}_1^f, \mathbf{e}_2^f, \mathbf{e}_3^f)$ of the fiber coordinate system are defined as follows:

$$\mathbf{e}_3^f = \frac{\mathbf{X}^{top} - \mathbf{X}^{bot}}{t} \quad \mathbf{e}_2^f = \frac{\mathbf{e}_3 \times \mathbf{e}_j}{\|\mathbf{e}_3 \times \mathbf{e}_j\|} \quad \mathbf{e}_1^f = \mathbf{e}_2 \times \mathbf{e}_3, \quad (23)$$

$t(\xi_1, \xi_2)$ is the thickness of the shell defined as,

$$t = \|\mathbf{X}^{top} - \mathbf{X}^{bot}\| \quad (24)$$

and $\mathbf{e}_j$ is chosen such that fiber reference frame is close to global Cartesian system [12].

For the purpose of discussion here the iso-parametric shell element discretization is viewed of consisting of the following two steps:

(1) Evaluate the displacement field at the finite element nodes ($\xi_1 = \xi_1^A$, $\xi_2 = \xi_2^A$) using eqn (22): $u_i^A(\xi_3) = u_i(\xi_1 = \xi_1^A, \xi_2 = \xi_2^A, \xi_3)$.
(2) Interpolate the displacement field using two-dimensional Lagrangian basis functions: $u_i(\xi_1, \xi_2, \xi_3) = N_A^{lag}(\xi_1, \xi_2) u_i^A(\xi_3)$.

The extension of this approach to the hierarchical p-method where degrees-of-freedom do not represent the value of the solution at a specific location within the element is not trivial. It involves sampling for the solution value at some arbitrary points, say, finite element nodes corresponding to Lagrangian interpolation followed by inverse mapping aimed at finding corresponding amplitudes of hierarchical modes. Unfortunately, for higher polynomial orders this will involve inversion of large element matrices, which may overshadow the benefit from a hierarchical degenerated shell element formulation.

In the present work we propose a different route by which the fields $u_i^t(\xi_1, \xi_2)$ and $\theta_\alpha(\xi_1, \xi_2)$ are directly discretized using Legendre polynomials. The resulting solution approximation takes the following form:

$$\begin{Bmatrix} u_1 \\ u_2 \\ u_3 \end{Bmatrix} = \sum_{A=1}^{NMDS} N_A(\xi_1, \xi_2) \begin{Bmatrix} u_1^{tA} \\ u_2^{tA} \\ u_3^{tA} \end{Bmatrix} + \sum_{A=1}^{NMDS} N_A(\xi_1, \xi_2) \frac{\xi_3}{2}[-t\mathbf{e}_2^f, t\mathbf{e}_1^f]_{(\xi_1,\xi_2)} \begin{Bmatrix} \theta_1^A \\ \theta_2^A \end{Bmatrix}. \quad (25)$$

Note that there is a fundamental difference between eqn (25) and its iso-parametric counterpart. In the classical iso-parametric formulation the variable vector functions $\mathbf{e}_i^f(\xi_1, \xi_2)$ in eqn (25) are replaced by a set of constant vectors $\mathbf{e}_i^f(\xi_1^A, \xi_2^A)$ representing the fiber coordinate system at the node A. The present formulation gives rise to an additional term Δ_A in the displacement gradient evaluation:

$$\frac{\partial \mathbf{u}}{\partial \xi_\alpha} = \sum_{A=1}^{NMDS} \frac{\partial N_A(\xi_1, \xi_2)}{\partial \xi_\alpha} \begin{Bmatrix} u_1^{tA} \\ u_2^{tA} \\ u_3^{tA} \end{Bmatrix} + \sum_{A=1}^{NMDS} \times \left[\frac{\partial N_A(\xi_1, \xi_2)}{\partial \xi_\alpha} \frac{\xi_3}{2}[-t\mathbf{e}_2^f, t\mathbf{e}_1^f] + \Delta_A \right] \begin{Bmatrix} \theta_1^A \\ \theta_2^A \end{Bmatrix} \quad (26)$$

and

$$\Delta_A = N_A(\xi_1, \xi_2) \frac{\xi_3}{2} \left[-\frac{\partial (t\mathbf{e}_2^f)}{\partial \xi_\alpha}, \frac{\partial (t\mathbf{e}_1^f)}{\partial \xi_\alpha} \right] \quad (27)$$

where $\alpha \in [1,2]$. Derivatives of $((t\mathbf{e}_1^f), (t\mathbf{e}_2^f))$ are obtained by differentiation of appropriate mapping functions:

$$\frac{\partial t}{\partial \xi_i} = \frac{1}{t}[(\mathbf{X}^{top} - \mathbf{X}^{bot}) \cdot (\mathbf{X}_{,\xi_i}^{top} - \mathbf{X}_{,\xi_i}^{bot})] \quad (28)$$

$$\frac{\partial \mathbf{e}_3^f}{\partial \xi_i} = \left[\frac{1}{t}(\mathbf{X}_{,\xi_i}^{top} - \mathbf{X}_{,\xi_i}^{bot}) - \frac{(\mathbf{X}^{top} - \mathbf{X}^{bot})}{t^2} \frac{\partial t}{\partial \xi_i} \right] \quad (29)$$

and from eqn (23) we have,

$$\frac{\partial \mathbf{e}_2^f}{\partial \xi_i} = \frac{1}{\|\mathbf{e}_3^f \times \mathbf{e}_j\|} \left(\frac{\partial \mathbf{e}_3^f}{\partial \xi_i} \times \mathbf{e}_j \right) - \frac{(\mathbf{e}_3^f \times \mathbf{e}_j)}{\|\mathbf{e}_3^f \times \mathbf{e}_j\|^3} \left\{ \mathbf{e}_3^f \cdot \frac{\partial \mathbf{e}_3^f}{\partial \xi_i} - \left(\frac{\partial \mathbf{e}_3^f}{\partial \xi_i} \cdot \mathbf{e}_j \right) (\mathbf{e}_3^f \cdot \mathbf{e}_j) \right\} \quad (30)$$

$$\frac{\partial \mathbf{e}_1^f}{\partial \xi_i} = \left(\mathbf{e}_2^f \times \frac{\partial \mathbf{e}_3^f}{\partial \xi_i} \right) + \left(\frac{\partial \mathbf{e}_3^f}{\partial \xi_i} \times \mathbf{e}_2^f \right). \quad (31)$$

Derivative w.r.t. ξ_3 is given as,

$$\frac{\partial \mathbf{u}}{\partial \xi_3} = \sum_{A=1}^{NMDS} [N_A(\xi_1, \xi_2)\tfrac{1}{2}[-t\mathbf{e}_2^I, t\mathbf{e}_1^I]] \begin{Bmatrix} \theta_1^A \\ \theta_2^A \end{Bmatrix}. \quad (32)$$

2.4.1. *Remarks.*

(2) The derivatives of $(t\mathbf{e}_1^I)$ and $(t\mathbf{e}_2^I)$ in the natural coordinate system can be precomputed in the preprocessing stage and thus the overhead associated with the computation of additional term Δ_A is not significant.

(3) Special care must be exercised to avoid derivatives of fiber vectors becoming unbounded in the element domain. For example, in a cylindrical surface with unit radius, where $x_1^2 + x_2^2 = 1$ and x_3 along the axis of the cylinder. The derivatives of the fiber vectors involve a term of the form $\partial\sqrt{1-x_1^2}/\partial x_1$ which becomes unbounded as $x_1 \to 1$. To avoid such situations the element is formulated in the local element coordinate system [14] and the size of a single element is restricted so that the included angle of the element is no greater than 90°.

2.5. *H2ANS—hierarchic (2 − D) degenerated assumed natural strain element with rotational degrees-of-freedom*

H2ANS represents a combination of H2SOL and H3ANS elements. It can be viewed as a hierarchical counterpart of four and nine node ANS elements [14]. The natural strain–Cartesian displacement matrix for this element is formulated on the basis of eqns (6) and (22):

$$\mathbf{B}_A = \begin{bmatrix} \mathbf{b}^u_{A_{11}} & \mathbf{b}^\theta_{A_{11}} \\ \mathbf{b}^u_{A_{22}} & \mathbf{b}^\theta_{A_{22}} \\ \mathbf{b}^u_{A_{33}} & \mathbf{b}^\theta_{A_{33}} \\ \mathbf{b}^u_{A_{23}} & \mathbf{b}^\theta_{A_{23}} \\ \mathbf{b}^u_{A_{12}} & \mathbf{b}^\theta_{A_{12}} \\ \mathbf{b}^u_{A_{13}} & \mathbf{b}^\theta_{A_{13}} \end{bmatrix} \begin{Bmatrix} d_1^A \\ d_1^A \\ d_3^A \\ \theta_1^A \\ \theta_2^A \end{Bmatrix} = [\mathbf{B}^u_A, \mathbf{B}^\theta_A] \begin{Bmatrix} d_1^A \\ d_1^A \\ d_3^A \\ \theta_1^A \\ \theta_2^A \end{Bmatrix} \quad (33)$$

where $\mathbf{B}^u_A$ is defined as in eqn (9) and $\mathbf{B}^\theta_A$ is given by:

$$[\mathbf{B}^\theta_A] = \begin{bmatrix} (N_{A,\xi_1}\omega_1 + N_A\omega_{11}) & (N_{A,\xi_1}\varphi_1 + N_A\varphi_{11}) \\ (N_{A,\xi_2}\omega_2 + N_A\omega_{22}) & (N_{A,\xi_2}\varphi_2 + N_A\varphi_{22}) \\ (N_{A,\xi_3}\omega_3 + N_A\omega_{33}) & (N_{A,\xi_3}\varphi_3 + N_A\varphi_{33}) \\ (N_{A,\xi_3}\omega_2 + N_A\omega_{32} + N_{A,\xi_2}\omega_3 + N_A\omega_{23}) & (N_{A,\xi_3}\varphi_2 + N_A\varphi_{32} + N_{A,\xi_2}\varphi_3 + N_A\varphi_{23}) \\ (N_{A,\xi_1}\omega_2 + N_A\omega_{12} + N_{A,\xi_2}\omega_1 + N_A\omega_{21}) & (N_{A,\xi_1}\varphi_2 + N_A\varphi_{12} + N_{A,\xi_2}\varphi_1 + N_A\varphi_{21}) \\ (N_{A,\xi_1}\omega_3 + N_A\omega_{13} + N_{A,\xi_3}\omega_1 + N_A\omega_{31}) & (N_{A,\xi_1}\varphi_3 + N_A\varphi_{13} + N_{A,\xi_3}\varphi_1 + N_A\varphi_{31}) \end{bmatrix} \quad (34)$$

where ω_j ω_{ij} and φ_j φ_{ij} are given as,

$$\omega_j = -1.0\{\mathbf{a}_j \cdot (t\mathbf{e}_2^I)\}$$

$$\omega_{ij} = -1.0\left[\mathbf{a}_i \cdot \left\{\frac{\partial(t\mathbf{e}_2^I)}{\partial \xi_j}\right\}\right]$$

$$\varphi_j = \mathbf{a}_j \cdot (t\mathbf{e}_1^I)$$

$$\varphi_{ij} = \mathbf{a}_i \cdot \left\{\frac{\partial(t\mathbf{e}_1^I)}{\partial \xi_j}\right\}.$$

Selective reduction in the polynomial order of natural strains is carried out in the similar fashion as for H3ANS element.

3. ADAPTIVITY AND QUALITY CONTROL

Both *a posteriori* error estimation scheme and adaptive strategy are based on hierarchical spectral order enrichment. One of the earliest uses of this approach was by Zienkiewicz and his associates in the early 1980s [15]. By this technique given the finite element solution $u^{p,A}$ corresponding to the finite element space $S^{(p,A)}$ one can hierarchically enrich the space by adding certain hierarchical basis functions to the set already used for $S^{(p,A)}$. If $S^{(p,A,l)}$ is the new space, then we have the hierarchical decomposition

$$S^{(p,A,l)} = S^{(p,A)} \oplus W^l \quad (35)$$

where W^l is the subspace which corresponds to the span of the additional basis functions and l is the list of additional basis functions.

Let the estimated error $\mathbf{E} = \phi\beta \in W^l$ be a linear combination of basis functions ϕ spanning the subspace W^l, then the unknown coefficients β are obtained by minimization of the energy functional on the subspace W^l, that is,

$$\tfrac{1}{2}[\mathbf{K}(\mathbf{u}^{p,A} + \phi\beta), (\mathbf{u}^{p,A} + \phi\beta)] - (\mathbf{f}, \mathbf{u}^{p,A} + \phi\beta) \to \min_{\beta} \quad (36)$$

where $\mathbf{K}$ and $\mathbf{f}$ are the stiffness matrix and the force vector corresponding to the enriched space $S^{(p,A,l)}$ and $(\cdot, \cdot)$ denotes the bilinear form given by

$$(\mathbf{u}, \mathbf{v}) = \sum_{j=1}^{n} u_j v_j. \quad (37)$$

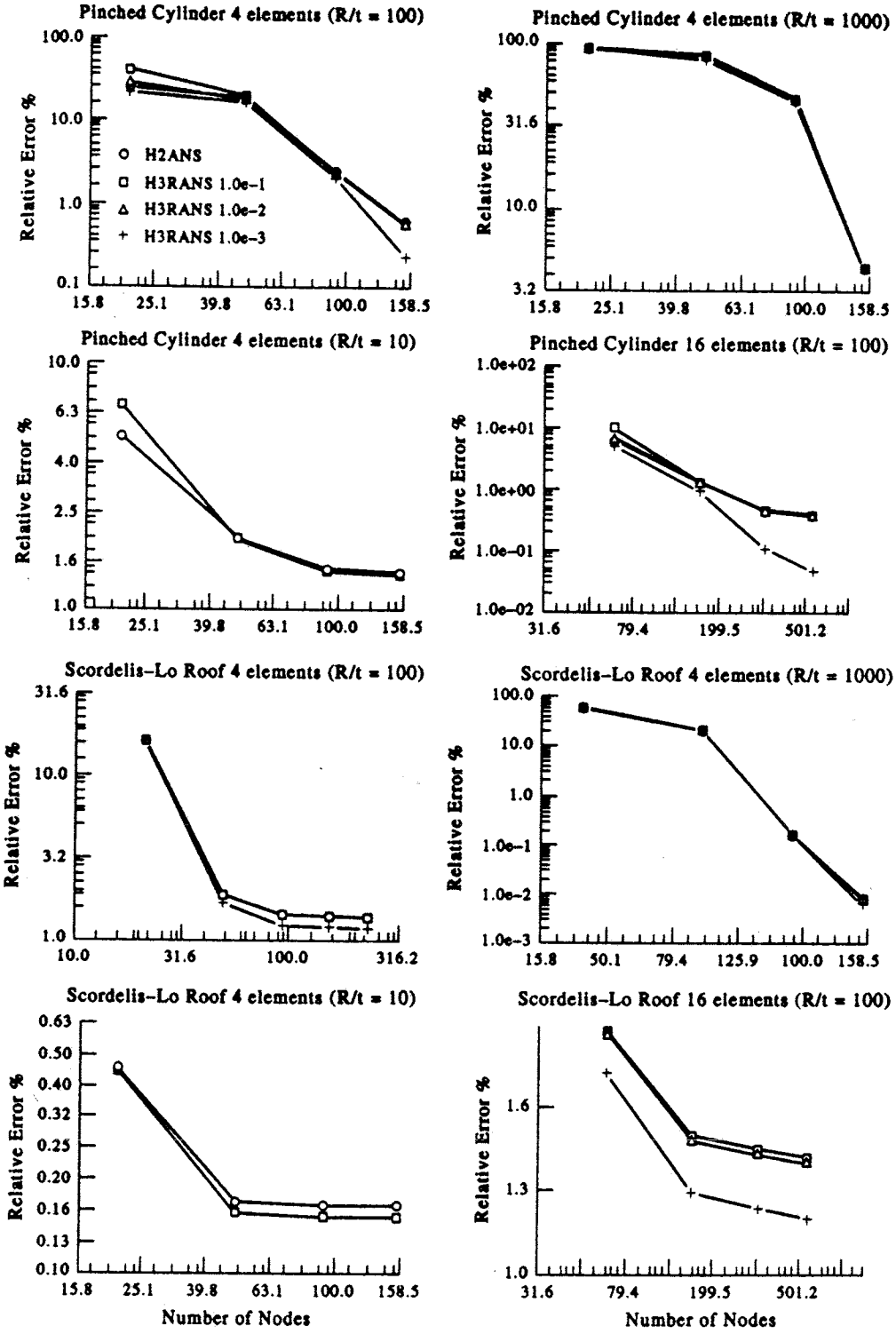

Fig. 1. Experimental rates of convergence for H2-type and H3R-type assumed natural strain elements.

Since the hierarchical basis functions ϕ are typically highly oscillatory functions with compact support, it is common practice to approximate the stiffness matrix corresponding to the subspace W^l by its diagonal form, which further reduces the cost of computing the error estimate. By this technique the error estimate in the energy norm is given by,

$$\|\mathbf{E}\| = \left[\sum_{\lambda=1}^{n} \eta_\lambda^2\right]^{1/2} \tag{38}$$

where

$$\eta_A = \tfrac{1}{2}\beta_A^2 K_{AA} \tag{39}$$

and K_{AA} is the stiffness coefficient corresponding to the degree-of-freedom A. η_A is termed as an error indicator which measures the decrease in error of the solution by adding a particular new degree-of-freedom. Adaptive strategy is steered by the magnitude of the error indicators. At each step we add all degrees-of-freedom corresponding to error indicators, such that

$$\eta_A > \gamma \eta_{\max}. \tag{40}$$

Parameter $\gamma \in [0, 1]$ controls the speed of convergence: if γ is zero, then we add all possible degrees-of-freedom; if γ is one, we add none.

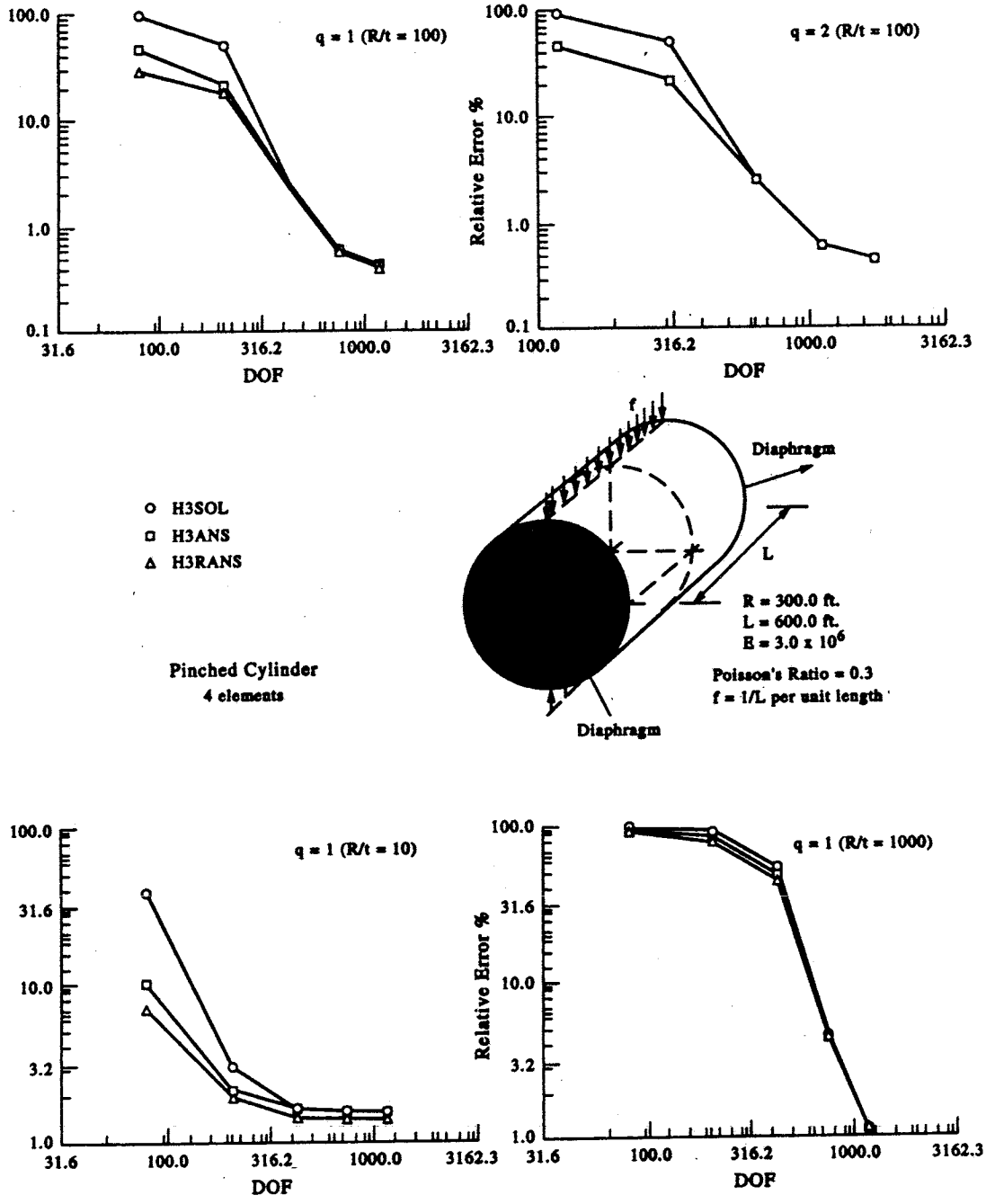

Fig. 2. Comparison of experimental rates of convergence for continuum and assumed strain H3-type elements for pinched cylinder.

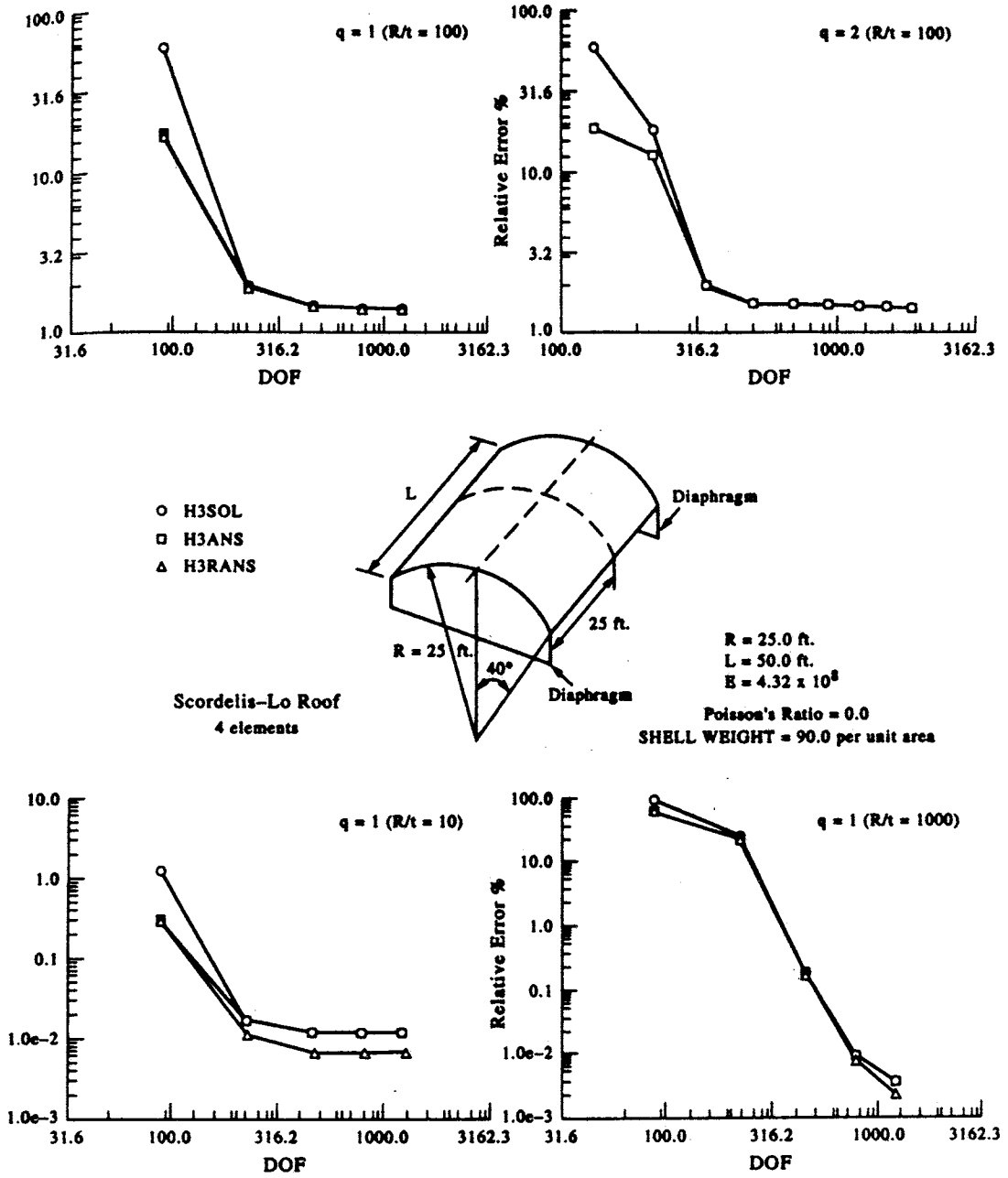

Fig. 3. Comparison of experimental rates of convergence for continuum and assumed strain H3-type elements for Scordelis-Lo roof.

The theoretical basis of the hierarchical *a posteriori* error estimator has been given by Bank and Smith [16]. They have shown that for self adjoint positive definite systems the estimated error in the energy norm is bounded by,

$$\frac{1}{C_1^2}\alpha\|\mathbf{u}-\mathbf{u}^{p,q}\|^2 \leq \|\mathbf{E}\|^2 \leq \frac{1}{C_0^2}\|\mathbf{u}-\mathbf{u}^{p,q}\|^2 \quad (41)$$

where $0 < \alpha < 1$ is a constant independent of the mesh size and the ratio C_1/C_0 represents the condition number of the stiffness matrix corresponding to the subspace W^1 preconditioned by its diagonal form.

Note that this theoretical framework is only valid as long as the finite element matrices are hierarchical, that is lower-order matrices are sub-matrices of higher-order matrices. Even though solution approximation is hierarchical the resulting finite element matrices will not be in the following three cases:

(1) Escalation of polynomial order in transverse direction from $q = 1$ to $q = 2$. Hierarchical

structure of matrices is lost as a result of change in the constitutive model from plane strress to a three-dimensional state of stress.

(2) Progressive change of geometry. Hierarchical structure of matrices is lost due to changing Jacobian matrix. In the present work for elements employing blending functions geometry mapping is fixed, while in the case of Lagrangian mapping we have studied the influence of simultaneously improving the quality of mapping with polynomial order escalation on the rate of convergence.

(3) Changing the quadrature scheme and assumed strain interpolation order for lower-order blocks.

Our experience indicates that the quality of error estimators and indicators as well as the efficiency of adaptive strategy could strongly degrade if the lower-order blocks are not recomputed in the three cases mentioned above.

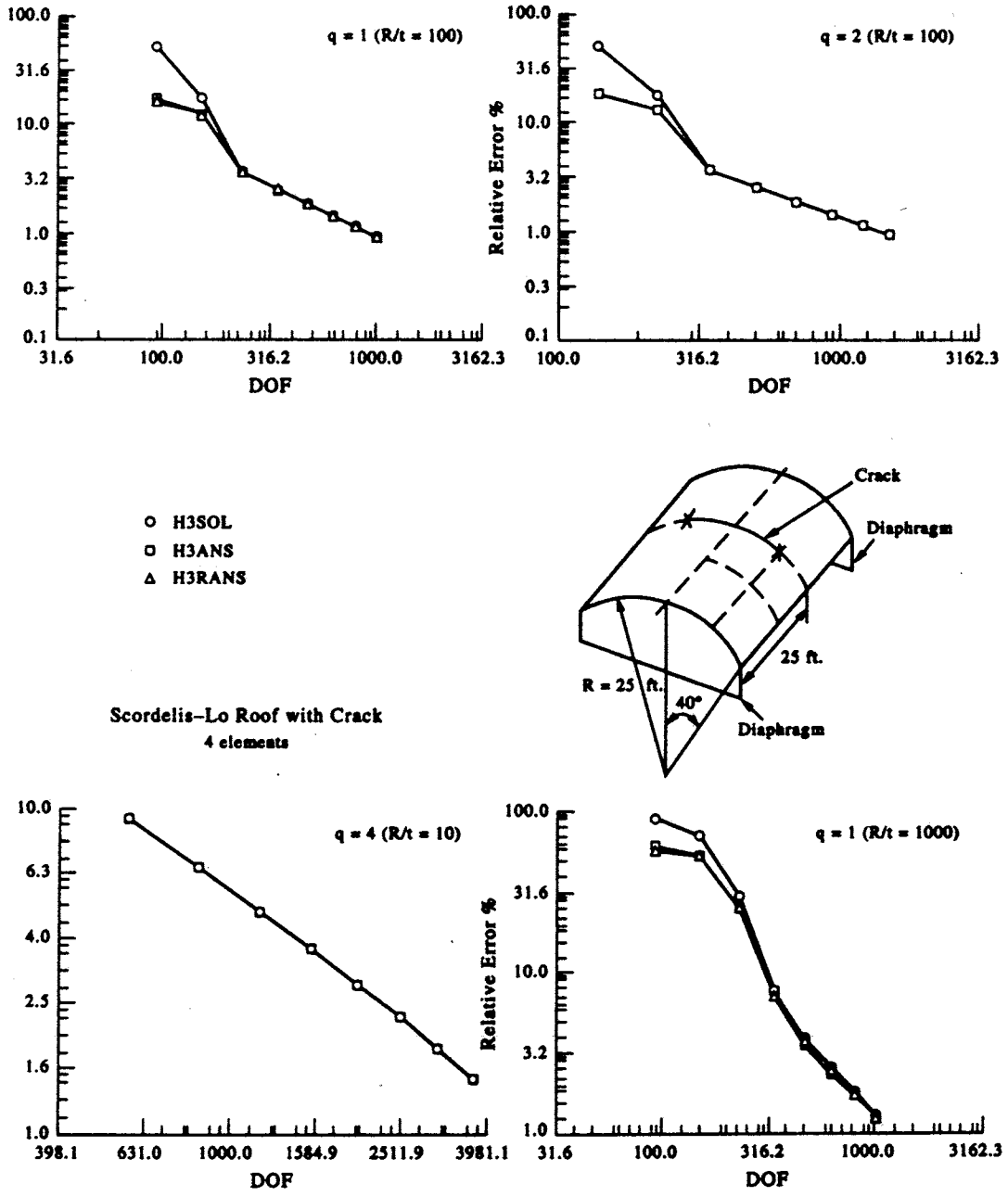

Fig. 4. Comparison of experimental rates of convergence for continuum and assumed strain H3-type elements for Scordelis-Lo roof with crack.

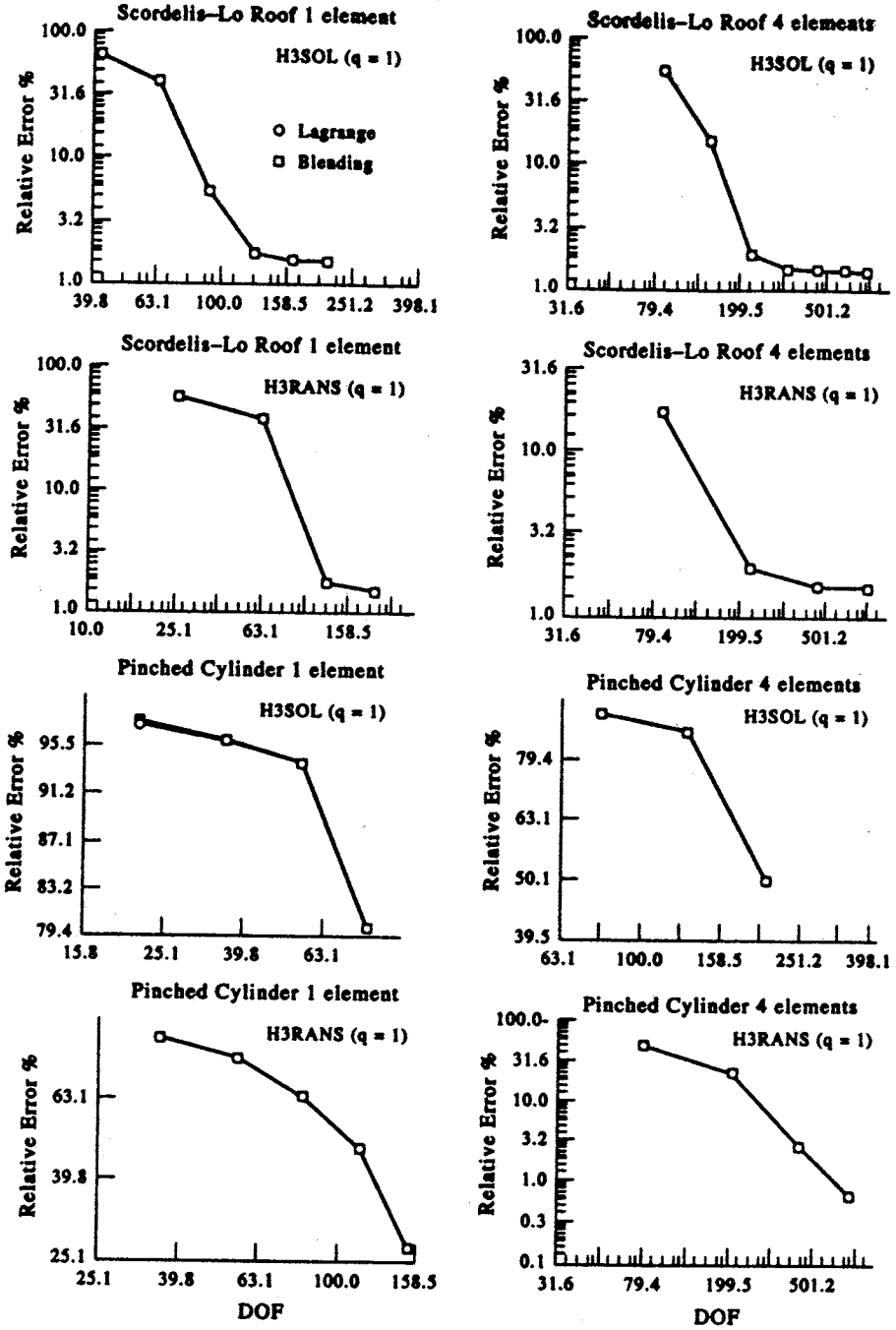

Fig. 5. Experimental rates of convergence for various elements with progressive (Lagrange) and fixed (blending) geometry.

4. NUMERICAL RESULTS

The performances of various hierarchical shell elements are compared in this section. The effects of assumed natural strain formulation, selective polynomial order escalation, the value of stabilization parameter for the transverse normal stiffness reduction, progressive change of geometry and mesh distortion on the rate of convergence are investigated. The following problems are considered,

- The pinched cylinder with rigid end diaphragms subjected to strip load (the width of the strip is equal to the thickness of the shell) as shown in Fig. 2. Due to symmetry only one eighth of the problem is solved.
- Scordelis-Lo roof loaded vertically by its own dead weight and supported by a rigid diaphragm at each end as shown in Fig. 3. A quarter of the problem is considered due to symmetry.

- Scordelis-Lo roof with crack problem is devised by introducing a crack in the Scordelis-Lo roof as shown in Fig. 4. Loading and essential boundary conditions are not changed.

For reference solution highly refined finite element meshes are considered. Percentage relative error is defined as:

$$\text{relative error} = \frac{U^{\text{ref}} - U^{\text{fe}}}{U^{\text{ref}}} \times 100 \qquad (42)$$

where U^{ref} and U^{fe} are the strain energy of the reference and FE solutions, respectively.

The influence of the value of stabilization parameter corresponding to transverse normal stiffness on the rate of convergence is presented in Fig. 1, which shows relative error vs total number of nodes (modes) in the mesh. For all the problems considered the results of H2ANS were in close agreement to those of H3RANS with the factor χ equal to h/l, where h and l are the smallest and largest dimensions of the shell element, respectively. It can be

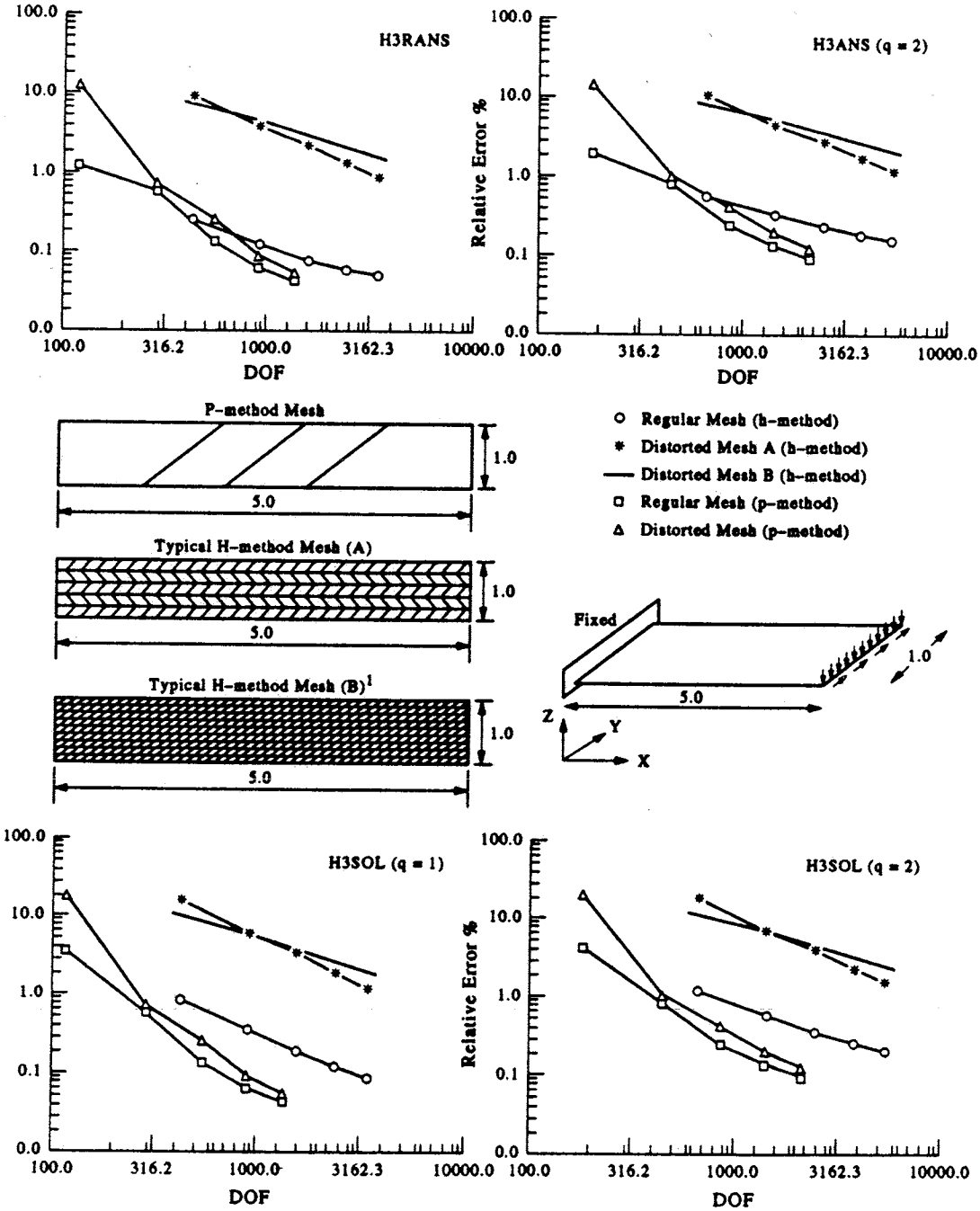

Fig. 6. Effect of mesh distortion on h- and p-versions of finite element method.

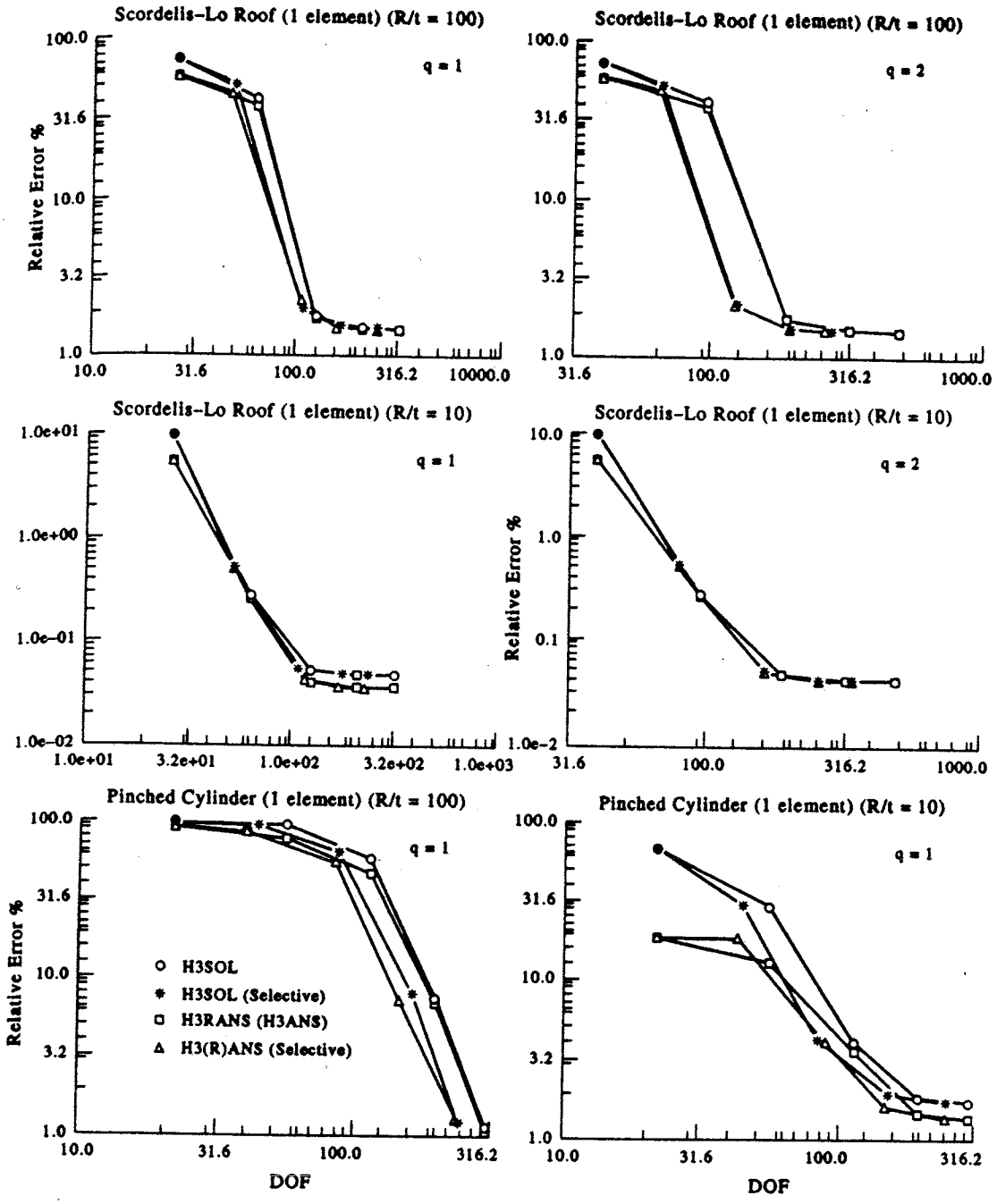

Fig. 7. Effect of selective refinement on rates of convergence for various H3-type elements.

seen that when $\chi \gg h/l$, the element H3RANS is stiffer and when $\chi \ll h/l$ it is softer. Nevertheless for the range of $\chi = 10^{-1}$–10^{-3} the element behavior was found to be close to that of the degenerated element with rotational degrees-of-freedom. Similar observations were found for H3RSOL and H2SOL elements. For subsequent numerical studies only H3RANS element with $\chi = h/l$ is considered.

The performance of elements H3RANS and H3ANS is compared with that of H3SOL in Figs 2–4. For the convergence studies relative error in the energy norm is plotted vs total number of degrees-of-freedom. Among the three elements H3RANS possesses the highest rate of convergence. For the test problems considered all elements give similar results for $p > 6$ where p is the in-plane polynomial order of basis functions. The only exception being the thick shells where H3RANS has somewhat better performance even for higher polynomial orders.

A comparison of the rate of convergence for elements with progressive geometry and fixed

geometry is depicted in Fig. 5. Progressive geometry mapping is carried out using Lagrange polynomials, the order of the Lagrange polynomials match that of the interpolation functions. Blending mapping functions are used for fixed geometry mapping. It is well known that for lower-order elements the super-parametric formulation degrades the element performance, since the rigid body modes are not represented exactly. It can be seen that for higher-order elements both approaches possess similar convergence.

The effect of mesh distortion is shown in Fig. 6. It is evident that mesh distortion degrades the performance of both p- and h-versions of finite element method, although the p-version was found to be less sensitive to mesh distortion.

The influence of selective polynomial escalation is studied in Figs 7 and 8. In general selective polynomial escalation leads to higher rates of convergence. This trend is more pronounced for higher values of q, where q is the polynomial order of interpolation functions in the transverse direction.

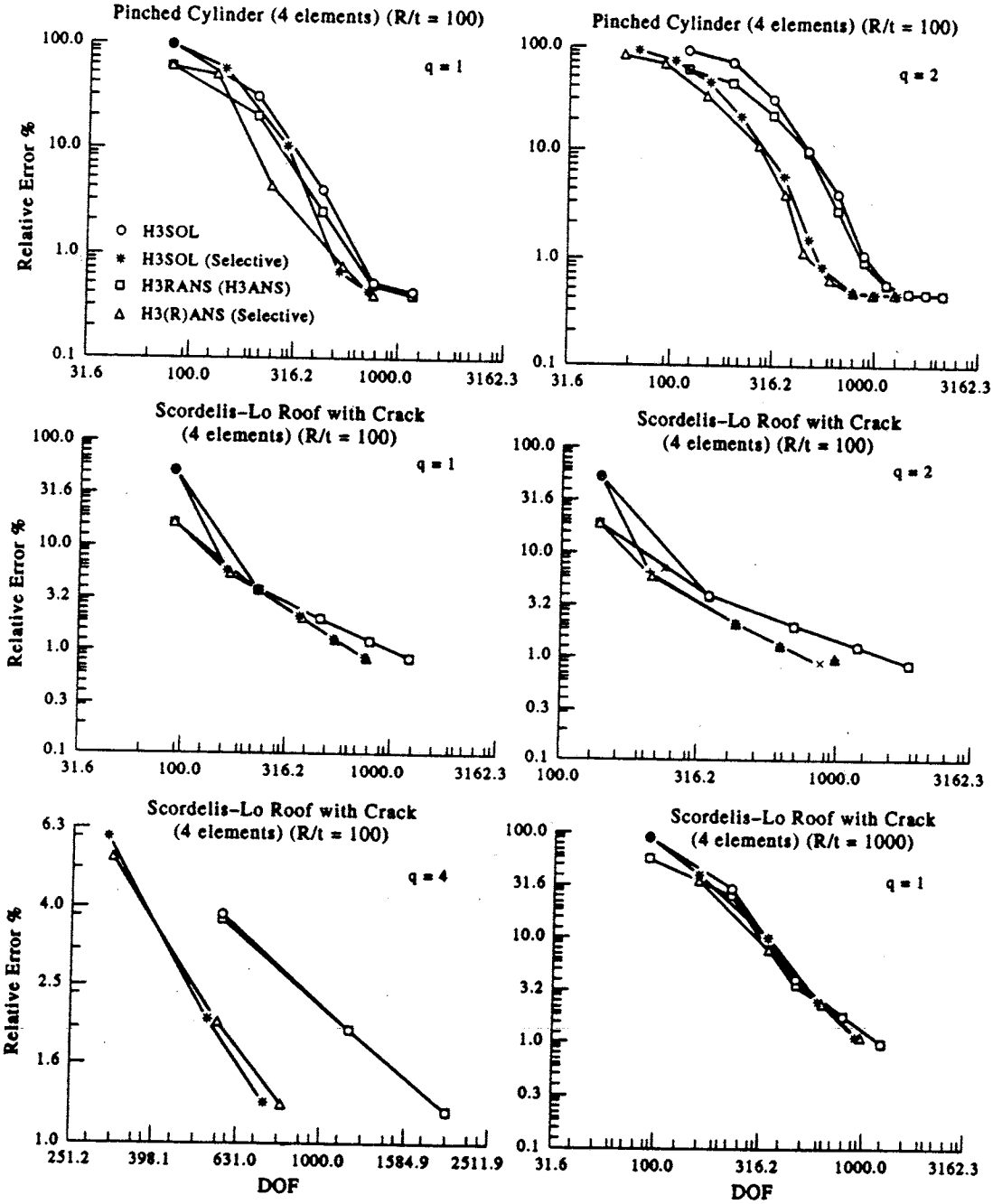

Fig. 8. Effect of selective refinement on rates of convergence for various H3-type elements.

5. CONCLUSIONS

A family of hierarchical assumed strain shell elements with selective polynomial order escalation has been developed. Several conclusions can be drawn:

- The usefulness of assumed strain formulation for hierarchical shells depends primarily on element size and accuracy requirements, that is, if the satisfactory accuracy can be achieved at polynomial orders ranging from two to five, then such formulation might be advantageous.
- Selective polynomial order escalation is highly recommended for thick shells with strong local effects, but its usefulness is limited to problems with one or very few right-hand sides.
- Higher-order shell elements are less sensitive to mesh distortion. Moreover, the super-parametric formulation, which significantly degrades the performance of lower-order elements, seems to have no influence on higher-order assumed strain and displacement-based elements.

REFERENCES

1. PROBE Theoretical Manual, release 1.0, Neotic Technologies Corp, 1985.
2. Babuska, I., Szabo, B. A. and Katz, I. N., The p-version of the finite element method. *SIAM Journal of Numerical Analysis*, 1981, **18**, 512–545.
3. Private communications, MSC/NASTRAN and Swanson Analysis, 1994.
4. Ramm, E., Stander, N. and Matzenmiller, A., An assessment of assumed strain methods in finite rotation shell analysis. *Engineering and Computers*, 1989, **6**.
5. Peano, A. G., Hierarchies and conforming finite elements for plane elasticity and plate bending. *Computers and Mathematics*, 1976, **2**, 211–224.
6. Surana, K. S. and Sorem, R. M., p-version hierarchical three-dimensional curved shell element for elastostatics. *International of Journal of Numerical Methods Engineering*, 1991, **31**, 649–676.
7. Szabo, B. A. and Sahrmann, G. J., Hierarchic plate and shell models based on p-extensions. *International of Numerical Methods Engineering*, 1988, **26**, 1855–1881.
8. Carnevali, P., Morris, R. B., Tsuji, Y. and Taylor, G., New basis functions and computational procedures for p-type finite element analysis, RJ 8710 (78272) Engineering Technology, April 3, 1992.
9. Lo, K. H., Christensen, R. M. and Wu, E. M., A higher-order theory of plate deformation. *Journal of Applied Mechanics*, 1977, **44**, 669–676.
10. Stanley, G. M., Levitt, I., Stehlin, B. and Hurlburt, B., Adaptive analysis of composite shell structures via thickness-tailored 3D finite elements. *Winter Annual Meeting, Anaheim*, CA, November 11–13, 1992.
11. Belytschko, T., Stolarski, H., Liu, W. K., Carpenter, N. and Ong, J. S-J, Stress projection for membrane and shear locking in shell finite elements. *Computational Methods in Applied Mechanics and Engineering*, 1985, **51**, 221–258.
12. Hughes, T. J. R., *The Finite Element Method*. Prentice-Hall, Englewood Cliffs, NJ, 1987.
13. Ahmed, N. U. and Basu, P. K., Higher-order modeling of plates by p-version of finite element method. *Journal of Engineering Mechanics, ASCE*, 1993, **119**, 1228–1242.
14. Park, K. C. and Stanley, G. M., A curved C^0 shell element based on assumed natural coordinates strains. *Journal of Applied Mechanics*, 1986, **108**, 278–290.
15. Zeinkiewicz, O. C. and Craig, A., Adaptive refinement, error estimates, multigird solution and hierarchic finite element method concepts. *In Accuracy Estimates and Adaptive Refinements Finite Element Computations*, eds I. Babuska, O. C. Zeinkiewicz, J. Gago and E. R. de A. Oliveira.
16. Bank, R. E. and Smith, R. K., *A posteriori* error estimates based on hierarchical bases. *SIAM Journal on Numerical Analysis* 1993, **30**, 921–935.
17. Fish, J., Markolejas, S., Guttal, R. and Nayak, P., On adaptive multilevel superposition of finite element meshes for linear elastrostatics. *Applied Numericol Mathematics*, 1994, **14**, 135–164.